Fermilab

Analysis of multipacting threshold sensitivity to the random distributions of the secondary electron yield parameters

FERMILAB-PUB-24-1025-TD

scientific reports

Check for updates

OPEN

Analysis of multipacting threshold sensitivity to the random distributions of the secondary electron yield parameters

Firozeh Kazemi[1], Maryam Mostajeran[1]✉ & Gennady Romanov[2]

The way multipacting develops, depends strongly on the secondary emission property of the surface material. The knowledge of secondary electron yield is crucial for accurate prediction of the multipacting threshold. Variations in secondary electron yield parameters from experimental measurements create uncertainty, stemming from handling and surface preparation, and these uncertainties significantly affect multipacting threshold predictions. Despite their significance, the previous studies on the multipacting phenomenon did not adequately address the effect of an assumed random distribution of the secondary emission parameters on the multipacting threshold. Therefore, this paper aims to provide a comprehensive statistical study on how the different random distributions of the secondary emission parameters and, as a result, the uncertainty in the secondary electron yield affect multipacting thresholds. We focus on three commonly used distributions, namely uniform, normal, and truncated normal distributions, to define the uncertainty of random inputs. We use the chaos polynomial expansion method to determine how much each of the random parameters contributes to the multipacting threshold uncertainty. Additionally, we calculate Sobol sensitivity indices to evaluate the impact of the individual parameters or groups of parameters on the model outputs and study how different random distributions of these parameters affected the Sobol index results.

High-power radio frequency (RF) devices operating under vacuum conditions are potentially susceptible to the occurrence of multipacting breakdown. Multipacting is an electromagnetic phenomenon primarily caused by secondary electrons in particle accelerators, microwave tubes, antennas, RF windows, and space equipment[1].

It is necessary to implement the practical measures to ensure the safe operation of RF devices and prevent multipacting discharge. Methods like third harmonic detection or phase vacuum detection can identify the multipacting discharge[2,3]. These methods can play an important role in assessing the risk of multipacting and ensuring proper device design. However, due to the high costs of these experimental methods, the theoretical approaches[4–6] and the numerical studies[7] are predominantly used to predict the multipacting threshold and achieve optimal design of RF devices. Therefore, the accuracy of multipacting threshold prediction may significantly affect the performance of RF devices. For accurate multipacting threshold prediction, it is necessary to consider the unavoidable secondary emission yield (SEY) variations associated with measuring the SEY data from the experimental samples with an uncertain history of handling and surface preparation. SEY is defined as the ratio of the number of secondary electrons (N_{sec}) to the incident or primary electrons (N_{inc}) on the material surface:

$$SEY = \frac{N_{sec}}{N_{inc}}. \tag{1}$$

Figure 1 shows the general behaviour of SEY as a function of the incident electron energy. There are several models of secondary emission, such as the Furman and Pivi[8], Vaughan[9], and Sombrin models[10], to describe the SEY versus the incident electron energy.

The SEY curve is determined by four key parameters: W_1 and W_2, which represent the crossover energy values at which SEY = 1, the maximum SEY value SEY_{max}, and W_{max}, the energy that corresponds to SEY_{max}.

[1]Faculty of Physics, Yazd University, P.O. Box 89195-741, Yazd, Iran. [2]Fermi National Accelerator Laboratory, Batavia, IL 60510, USA. ✉email: mostajeran@yazd.ac.ir

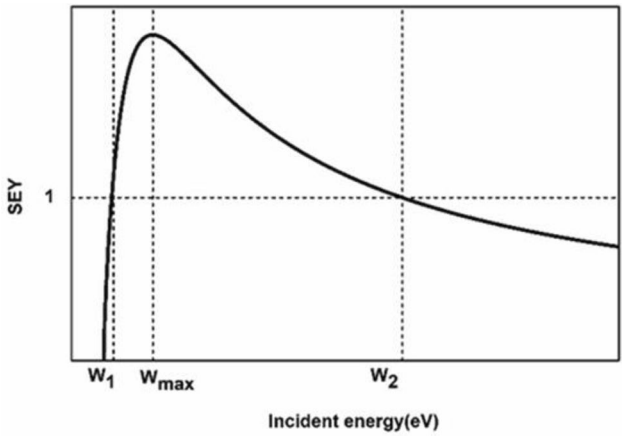

Figure 1. The behaviour of the secondary electron yield (SEY) with respect to the incident electron energy.

Measuring the SEY as a function of incident energy is a surface-sensitive process. The measured SEY values are highly influenced by the treatment of material surfaces prior to entering the vacuum. Despite the efforts to maintain repeatability in many SEY measurements, the significant uncontrolled variables during these measurements can lead to discrepancies between reported and actual values. Factors such as exposure to air, ambient temperature, cleanliness of measurement equipment, and other variables can create deviations in SEY measurements[11], and it is important to consider these variations when analyzing and interpreting SEY data. For example, the experimental observations have shown that exposure to air and subsequent oxidation can increase SEY_{max} of metals beyond their nominal values, typically ranging from 1 to 2, to values greater than 3[12]. Additionally, a surface layer of chemical pollution, which often forms after exposure to air, can also induce changes in SEY[13]. In other words, the reported SEY values have the uncertainties that contribute to the multipacting threshold uncertainty.

Uncertainty Quantification (UQ) methods such as generalized Polynomial Chaos expansion (gPC) can analyze how input uncertainties affect system performance and lead to more efficient RF system design and construction. In the RF systems the dielectrics are also widely used along with the metals and they are susceptible to multipacting occurrence due to the high SEY. The most typical example of dielectric usage is ceramic for vacuum RF windows[14–17]. On the disk type ceramic vacuum RF windows usually single-sided multipacting occurs. This article investigates the sensitivity of the threshold for single-sided multipacting on dielectrics. In this type of multipacting, the electrons are emitted from and collide with the same surface. For the mentioned disk, ceramic window, the single-side multipacting involves two fields: the RF electric field parallel to the dielectric surface (E_{RF}), which accelerates the emitted electrons and the DC electric field perpendicular to the surface (E_{DC}), which returns the electrons back to the surface of dielectric. Simulations of the single-side multipacting are often performed using a simplified flat surface model, as the results can be extrapolated to models that are more complex. A detailed description of the mechanism of single-sided multipacting can be found in Ref.[18]. In this paper, we use the PIC PARTICLE STUDIO module from the CST Studio Suit software to simulate the multipacting phenomenon using the simplified model. The initial conditions and physical parameters utilized in the simulations are presented in Table 1.

So far, most of the multipacting studies focused on investigating multipacting mechanisms[19,20], developing prediction techniques[21,22], and mitigating this phenomenon using surface treatments[23]. However, limited analysis has examined how the uncertainties of the SEY parameters affect the multipacting threshold evaluation. In Ref.[24], the impacts of uncertainties of W_1 and SEY_{max} on the multipacting in SRF gun with triangular grooved surface were studied, the Furman model was used to describe the SEY. In Ref.[25], the authors have examined the uncertainty of W_1 and W_{max}, and its impact on the multipacting threshold for dielectrics, employing the Sombrin model for SEY calculation. Both studies assumed a uniform distribution when considering uncertainties SEY parameters. This choice is often made in uncertainty quantification studies for simplicity. However, given the inherently random nature of these parameters, it is important to examine how different types of uncertainty distributions can affect the analysis of multipacting thresholds. Investigation of different distributions of uncertainty in SEY parameters can help us to make more accurate predictions of the multipacting threshold. In the current study, we consider the uncertainties in the three main parameters of SEY – W_1, SEY_{max}, and W_{max} – making it more comprehensive than previous studies that typically consider only one or two parameters. Table 2 provides the surface characteristics, including the material and values of SEY parameters of the proposed simple model.

Frequency	Initial energy	E_{DC}	E_{RF}
325 MHz	7.5 eV	12 kV/m	20.250 kV/m

Table 1. Physical characteristics and initial conditions of the model.

Material	W_1 (eV)	W_{max} (eV)	SEY_{max}
Teflon128	22	380	2.3

Table 2. Surface characteristics of the model.

We employ the Sombrin model to calculate SEY as a function of incident energy, because the Sombrin model contains the three main SEY parameters (W_1, SEY_{max} and W_{max}) in its formulation. Additionally, the results from this model are close to the experimental data[26]. The table of the SEY data obtained with this model was imported into the CST PIC STUDIO to be used as imported secondary emission model.

In Sect. "Methodology" of this article, we will provide detailed description of the employed methodology, including an overview of the research process and the gPC approach. In Sect. "Calculating the multipacting threshold in CST software", we will discuss an index for determining the multipacting threshold by the CST software. In Sect. "Results", we will present the results of the univariate uncertainty, including investigation of uncertainty of W_1, SEY_{max}, and W_{max} with three different distributions. Furthermore, the results of the bivariable uncertainty, with three different distributions, will be also presented in this section. Bivariable uncertainty includes uncertainty of W_1&W_{max}, W_1&SEY_{max}, and SEYmax & W_{max}. A variance based global sensitivity analysis is performed to determine which SEY parameters have the greatest influence on multipacting threshold, and the results of this analysis will be presented. Finally, the conclusion Sect. "Conclusion" provides a summary of the overall findings of the paper.

Methodology

Research process

Identifying distributions for SEY parameter uncertainties

The normal, uniform and truncated normal distributions are selected to model the uncertainties of the W_1, SEY_{max} and W_{max} parameters.

Determining the random parameters

The three main SEY curve parameters—W_1, SEY_{max} and W_{max}—are considered as input random variables.

Defining the values of uncertainty

The uncertainty values are calculated using the relative standard deviation (σ_r), defined as the ratio of the standard deviation (σ) to the mean of the parameter values (μ). Three values of uncertainty corresponding to $\sigma_r = 5$, 10, 30% are considered for each SEY parameter.

Investigation framework for analyzing multipacting

Multipacting simulations are performed for each random parameter separately for each uncertainty value and distribution. The gPC method is employed to calculate the $\langle SEY \rangle$ function and multipacting threshold. Uncertainties in bivariable combinations (W_1&W_{max}, W_1&SEY_{max} and SEY_{max} & W_{max}) are also modeled as bivariate uncertainties. This process is represented in Fig. 2.

The gPC method

The gPC technique was first introduced by Ghanem and Spanos for solving several engineering problems[27]. This method represents the output as a polynomial expansion in terms of orthogonal polynomials that are functions of the input parameters. The coefficients of the polynomial expansion are determined by projecting the output onto the basic functions of the orthogonal polynomials. The resulting polynomial approximation can be used to estimate the statistical quantities of the output, such as the mean and the variance, and to propagate the uncertainty of the input parameters to the output. Here, we describe the main steps of the gPC technique, which we applied to our modelling of the multipacting threshold uncertainty in this study.

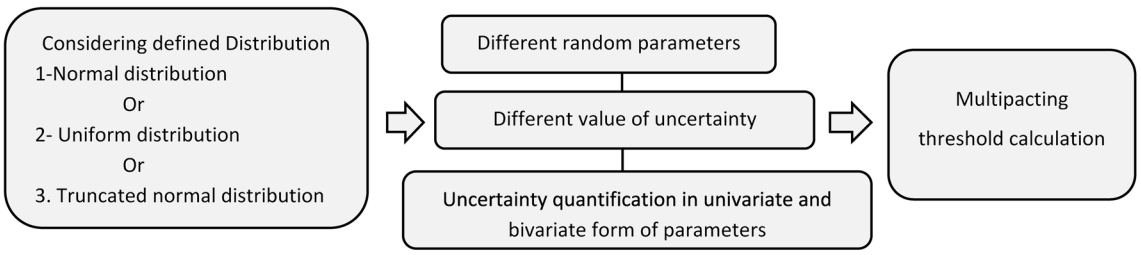

Figure 2. Research process in investigating the impact of random distribution of SEY parameters uncertainties on multipacting threshold uncertainty.

Generation polynomial chaos

In the gPC method, the type of polynomial chaos depends on the probability distribution of the random parameters. Some polynomials according to the type of random distributions are shown in Table 3.

In our study, we consider uniform, normal and truncated normal distribution for random parameters, so according to Table 3 we should use Legendre and Hermit polynomial respectively.

Normal distribution. A random variable $X \sim N(\mu, \sigma^2)$ follows a normal distribution. This distribution is characterized by two parameters: the mean (μ), which represents the center of the distribution, and the variance (σ^2), which determines the spread of the distribution. A random variable x with mean $\mu = 0$ and standard deviation $\sigma = 1$ is said to be a standard normal random variable and is denoted as $X \sim N(0, 1)$.

Uniform distribution. A random variable $X \sim U[a, b]$ follows a uniform distribution. The parameters "a" and "b" represent the lower and upper boundaries of the defined interval, respectively, wherein the probability of each event occurring is equal. The uniform distribution is the simplest form of continuous probability distribution. The case where $a = 0$ and $b = 1$ is the standard uniform distribution.

Truncated normal distribution. The truncated normal distribution is a probability distribution obtained by constraining the normal distribution within a specific range and the values outside this specific range are truncated. The parameters of the truncated normal distribution are the same as those of the normal distribution: the mean (μ) and the variance (σ^2), but with the additional specification of a range [a, b] for allowable values.

Generation the polynomial expansion

The basis of the gPC approach is to provide a polynomial surrogate for the computational model. In this context, the polynomial expansion represents the relationship between the system's response (Y) and the independent input parameters ξ in an M-dimensional space. The polynomial expansion can be expressed as following:

$$Y = \sum_{|\alpha| \leq N} C_\alpha \varphi_\alpha(\vec{\xi}). \tag{2}$$

where N is the degree of the polynomial expansion, α is the multi-index that indicate the degree of the polynomial in each of the input variables, C_α are the unknown coefficients to be determined and $\phi_\alpha(\vec{\xi})$ represents the multivariate polynomial. In our investigation, the system response we are interested in, is the multipacting threshold, and we aim to approximate a function representation for this quantity.

Determination of expansion coefficients

The coefficients, C_α, are determined by projecting the truncated expansion of Y on each basis polynomial and exploiting its orthogonality in the domain I:

$$C_\alpha = \langle \frac{1}{\phi_\alpha(\vec{\xi})\phi_\beta(\vec{\xi})} \rangle \int_I Y(\vec{\xi})\phi(\vec{\xi})D(\vec{\xi})d\vec{\xi}. \tag{3}$$

where $D(\vec{\xi})$ is the probability density function (PDF) of the random parameters. α and β are the multi-indices that indicate the order of the polynomial in each of the input variables. There are many methods for numerically multidimensional integration or quadrature, which is a classical problem.

In mathematics and numerical analysis, quadrature is an approximate method for computing integrals. Table 4 illustrates the comparison of integration techniques or quadrature and their respective integration points for three different random distributions.

The first column in Table 4 presents the types of distributions along with the corresponding polynomial quadrature method used. The "n = integration points" column represents the number of integration points utilized for each method. The second and third rows demonstrate the integration techniques applied to different distributions/polynomial. The Clenshaw-Curtis method is employed for the Uniform/Legendre distribution with 2^{N+1} integration points[29].

Numerical integration methods, such as quadrature, are employed to calculate these coefficients.

For detailed information on integration techniques and their application to different random distributions, refer to Table 4.

I	Distribution type orthogonal basis polynomial	Distribution orthogonal
$(-\infty, \infty)$	Hermit	Normal
$[-1, 1]$	Legendre	Uniform
$[0, 1]$	Jacobi	Beta
$(-1, 1)$	Laguerre	Exponential

Table 3. Distributions types and orthogonal basis polynomial support ranges I[28].

Distribution/polynomial	Quadrature	$\langle \Phi_\alpha(\xi)\Phi_\beta(\xi)\rangle = \delta_{\alpha\beta}\gamma_\alpha$	n = integration points
Uniform/Legendre	Clenshaw–Curtis[29–31]	$\gamma_\alpha = \frac{2}{2\alpha+1}$	2^{N+1}
Normal/Hermit	Gussi-Hermit	$\gamma_\alpha = \sqrt{\pi}2^\alpha \alpha!$	N + 1
Truncated normal/Hermit	Gussi-Hermit	$\gamma_\alpha = \sqrt{\pi}2^\alpha \alpha!$	N + 1

Table 4. Comparison of integration techniques, polynomial quadrature and with integration for different random distribution.

Transformation for random variables. Since Y depends on the parameter X, a transformation must be determined and the standard random variable ξ_i is mapped onto the random variable X_i. For example in our study, we interest in the deviation interval of W_1, SEY_{max} and W_{max}. We used the inverse transform method, which relies on the principle that continuous cumulative distribution functions (CDFs) are uniform in the interval [1, 0][32]. Here in, Table 5, we provide the transformation equations, integration points, and ranges of parameter deviations for $\sigma_r = 5\%$, 10%, and 30% of W_1.

To compute the coefficients C_N in Eq. (3) and, consequently, approximate the Y, the deterministic model is evaluated at sparse grid nodes.

Accuracy assessment

For accuracy assessment of the gPC, a posteriori error estimate approach is used to calculate the relative error for the (N + 1)st order of the gPC. In this study, we estimated this relative error using expansion coefficients. The formula related to the relative error is provided in Appendix A.

Global sensitivity analysis (Sobol's indices)

Sensitivity analysis assesses the influence of uncertain inputs parameters and interactions on the output variable (Y). A global, variance-based approach is valuable for customizing models by identifying inputs with minimal impact and quantifying the potential reduction in output uncertainty if these inputs were known. To achieve these objectives, Sobol introduce global, variance-based sensitivity indices[33].

The first-order Sobol sensitivity index, also referred to as the main sensitivity index, quantifies the portion that X_i contributes directly (without interaction) to the total variance of the output V[Y]. It aids to the identification of uncertain inputs that could be more precisely evaluated, thus facilitating input prioritization. The index is defined by Eq. (4);

$$S_i = \frac{V_{X_i}}{V}, \tag{4}$$

where V_{Xi} represents the variance associated with the f (X_i) and V is the total output variance.

Second-order sensitivity indices represent the portion of variance resulting from X_i and X_j interaction, they are defined as Eq. (5);

$$S_{i,j} = \frac{V_{X_i,X_j}}{V}. \tag{5}$$

$V_{Xi, Xj}$ represents the variance associated with the Y (X_i, X_j).

More details about the steps of the gPC technique are given in the Appendix A.

Distribution type	Standard range of ξ_i	Transformation equation	σ_r in W_1	Deviation interval of $W_1 = 22$ (eV)
Uniform	$\xi_i \sim U[-1, 1]$	$X_i = \frac{b-a}{2}\xi_i + \frac{b+a}{2}$	5%	$X_i \sim U[a = 20.9, \mu = 22, b = 23.11]$
			10%	$X_i \sim U[a = 19.8, \mu = 22, b = 24.2]$
			30%	$X_i \sim U[a = 15.4, \mu = 22, b = 28.6]$
Normal	$\xi_i \sim N(\mu = 0, \sigma = 1)$	$X_i = \mu + \sigma\xi_i$	5%	$X_i \sim N(\mu = 22, \sigma = 1.1)$
			10%	$X_i \sim N(\mu = 22, \sigma = 2.2)$
			30%	$X_i \sim N(\mu = 22, \sigma = 6.6)$
Truncated normal	$\xi_i \sim N(\mu = 0, \sigma = 1)$	$X_i = \mu + \sigma\xi_i$	5%	$X \sim N(\mu = 22, \sigma = 1.1, a = 20.9, b = 23.11)$
			10%	$X_i \sim N(\mu = 22, \sigma = 2.2, a = 19.8, b = 24.2)$
			30%	$X_i \sim N(\mu = 22, \sigma = 6.6\ a = 28.6, b = 28.6)$

Table 5. Standard range of ξ and range of deviation for $\sigma_r = 5\%$, 10%, 30% of $W_1 = 22$ (eV).

Calculating the multipacting threshold in CST software

The multipacting threshold refers to the combination of the system/model parameters at which multipacting discharge begins. In this study, the effects of space charge are not taken into account. Typically, in Multipacting simulations without space charge effects, the increase of the number of particles exhibits exponential behavior. However, there are instances where this assumption does not hold true; in such cases, the concept of the effective secondary electron yield is used as an index for the multipacting threshold. This parameter is not influenced by the specific manner in which the number of particles grows over time. As a result, it serves as a more robust and reliable indicator for Multipacting occurrence[34].

By formal definition, the effective secondary electron yield $\langle SEY \rangle$ is the ratio of the average number of secondary particles emitted from the surface to the average number of incident particles. In the context of this study, $\langle SEY \rangle$ serves as an indicator of the multipacting threshold. Specifically:

$\langle SEY \rangle > 1$: implies the occurrence of multipacting.

$\langle SEY \rangle = 1$: signifies the onset of multipacting.

$\langle SEY \rangle < 1$: indicates the absence of multipacting.

In CST software, it is more convenient to define $\langle SEY \rangle$ via currents, i.e. SEY is calculated as:

$$\langle \mathrm{SEY} \rangle = \frac{\langle \mathrm{I_{emission}} \rangle}{\langle \mathrm{I_{collision}} \rangle}, \tag{6}$$

where $\langle \mathrm{I_{emission}} \rangle$ and $\langle \mathrm{I_{collision}} \rangle$ are the emission and collision currents averaged over the last three RF periods of the simulation time. The sufficiently long simulation time allows the system to reach a developed and stable multipacting process, which improve the accuracy and robustness of our results. The averaging in its turn mitigates noise and fluctuations. All the operations are performed within post-processing tool of the CST software.

With the E_{DC} value of 12 kV/m, we performed multipacting simulations across various E_{RF} ranges to determine the radio frequency field amplitude required to reach the multipacting threshold. However, it should be noted that the CST software does not provide sufficiently high precision for obtaining the value of $\langle SEY \rangle = 1$ exactly. For the E_{RF} field amplitude of 20.250 kV/m, we considered the onset of multipacting to occur at $\langle SEY \rangle = 1.0065$, accurate up to two decimal places.

In Fig. 3, we have plotted the particle numbers versus time for $W_1 = 22$ eV and some deviations of this reference value of it. We observed that when the number of particles increases over time, the value of $\langle SEY \rangle$ increases to 1.01, and this indicates the occurrence of multipacting. Therefore, in this study, we considered the occurrence of multipacting when $\langle \mathrm{SEY} \rangle \geq 1.01$.

Results

Univariate uncertainty quantification results

Uncertainty of W_1

First, we examined the effect of uncertainty of W_1 (its nominal value is 22 eV) on $\langle SEY \rangle$, using the gPC method with three distributions: uniform, normal, and truncated normal. We modeled the uncertainty values by calculating the standard deviation quantity (σ_r) as 5%, 10%, and 30%. In our analysis, we assumed constant values for W_{max} (380 eV) and SEY_{max} (2.3).

We extended the approximation of the function to the expansion degree for which the calculated relative error of $\langle SEY \rangle$ becomes less than 0.25% as it was also employed in the reference[24]. In Fig. 4a and b, the relative error at different expansion degrees for normal and uniform distributions is illustrated respectively.

From the Fig. 4a and b, the relative error $\langle SEY \rangle$ for the uncertainty of 30% reduced below 0.25% for the 7th and 5th expansion degree for uniform and normal distribution respectively. Therefore, 7th and 5th expansion degrees have been chosen for subsequent evaluations.

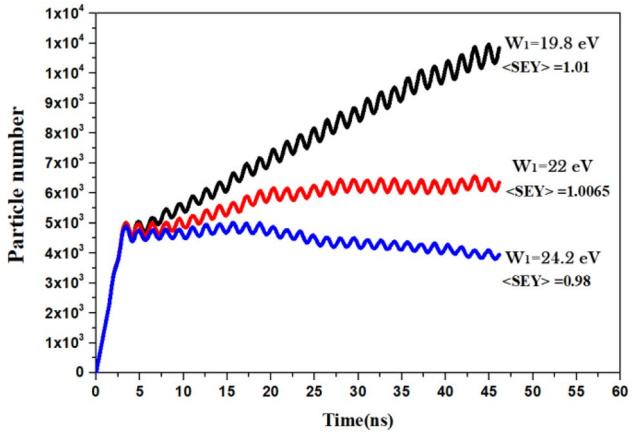

Figure 3. Particle number versus time.

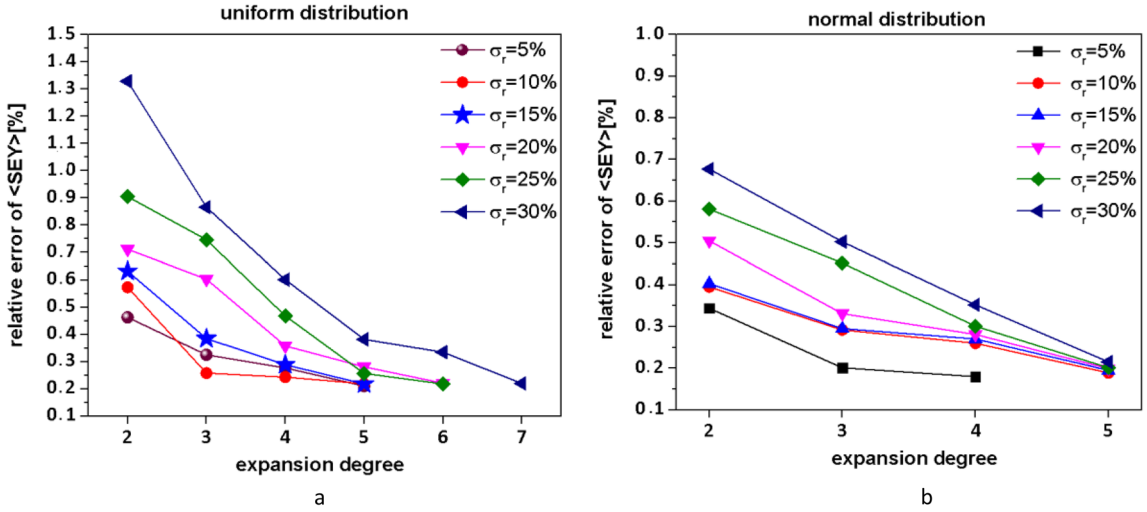

Figure 4. Relative errors versus expansion degrees, for inputs with, (**a**) uniform distribution by Clenshaw-Curtis quadrature, (**b**) normal distribution by Gussi-Hermit quadrature.

The uncertainty modeling and calculations were performed using the Python programming language in conjunction with the CST software. The statistical quantities related to the calculated values of $\langle SEY \rangle$ for $\sigma_r = 5$, 10, 30% of W_1 are presented in Table 6 including the following quantities:

- The expansion degree
- The average value of $\langle SEY \rangle$ is denoted as μ.
- The standard deviation is represented as σ.
- The variance is indicated as Var.
- The percentage change for μ of $\langle SEY \rangle$ compared to the multipacting threshold value is calculated as:

$$\langle SEY \rangle_{error} = \left(\frac{\mu - 1.0065}{1.0065} \right) \times 100 \tag{7}$$

- The results in Table 6 indicate that the multipacting threshold (μ of $\langle SEY \rangle$) remains unchanged up to two decimal places in the cases of $\sigma_r = 5$, 10%, of W_1 with any distribution. However, with an increase of the σ_r of W_1 up 30%, the multipacting threshold changes for the normal and uniform distributions, while it remains unchanged for the truncated normal distribution.
- The dispersion of $\langle SEY \rangle$, that measured by σ and Var, is approximately equal for the uniform and truncated normal distributions of W_1 with $\sigma_r = 5$, 10%. Moreover, this dispersion is lower compared to the normal distribution. With increased σ_r of W_1 up to 30%, the dispersion of $\langle SEY \rangle$ became higher for the uniform distribution than the truncated normal distribution. However, the normal distribution still exhibits the highest values of σ and Var, indicating that it possesses the greatest inherent dispersion of $\langle SEY \rangle$.
- In the cases of $\sigma_r = 30\%$ of W_1, $\langle SEY \rangle$ is significantly higher in the normal distribution than in the other two distributions.

σ_r of W_1	Distribution type	Expansion degree	μ of $\langle SEY \rangle$	$\langle SEY \rangle_{error}$	σ of $\langle SEY \rangle$	Var of $\langle SEY \rangle$
5%	Uniform	5	1.0069	0.03	0.0157	1.30E–04
	Normal	4	1.0064	0.02	0.0220	4.85E–04
	Truncated normal	4	1.0062	0.04	0.0116	1.34E–04
10%	Uniform	5	1.0070	0.04	0.0214	5.88E–04
	Normal	5	1.0087	0.21	0.0430	1.85E–03
	Truncated normal	5	1.0067	0.01	0.0242	5.85E–04
30%	Uniform	7	1.0270	2.03	0.0922	0.0056
	Normal	5	1.0383	3.15	0.1412	0.0199
	Truncated normal	5	1.0088	0.14	0.0468	0.0022

Table 6. Statistical quantities of $\langle SEY \rangle$ for different σ_r of W_1 with different distributions.

We have shown comprehensive results, which include the evaluation of three additional levels of uncertainty (σr = 15%, 20%, 30%) of W_1, in Table B1 in Appendix B.

Uncertainty of SEY_{max}
In this section, we examine the impact of uncertainty of $SEY_{max} = 2.3$. Following the same approach used in the previous section, we keep $W_{max} = 380$ eV and $W_1 = 22$ eV constant. The corresponding statistical quantities of $\langle SEY \rangle$ are presented in Table 7, for $\sigma_r = 5, 10, 30\%$ of SEY_{max}.

- According to the Table 7, for $\sigma_r = 5, 10$ of SEY_{max}, μ of $\langle SEY \rangle$ does not change significantly for any of the distributions. This implies the multipacting threshold remains unchanged at these lower uncertainty amounts. However, for $\sigma_r = 30\%$ of SEY_{max}, μ of $\langle SEY \rangle$ for all three distributions increases, that indicates a change in the multipacting threshold at the higher uncertainty amounts ($\sigma_r = 30\%$) of SEY_{max}.
- σ and Var values for the normal distribution are higher compared to the uniform and truncated normal distributions for the all uncertainty amounts ($\sigma_r = 5, 10, 30\%$).
- An important point is that the differences in results (in terms of μ, σ, Var of $\langle SEY \rangle$ and $\langle SEY \rangle_{error}$) for the different distributions of the SEY_{max} are relatively smaller when compared to the differences observed for the distributions of W_1 in the previous section.

A more comprehensive set of results is included in Appendix B, including the assessment of three additional uncertainty levels (σ_r=15%, 20%, 30%) of parameters SEY_{max} in Table B2.

Uncertainty of W_{max}
In this section, we investigate the impact of uncertainty of the W_{max} (its nominal value is 380 eV) on $\langle SEY \rangle$ with three different distributions. For this analysis, we keep the parameters SEY_{max} and W_1 constant at 2.3 and 22 eV, respectively. Table 8 presents the statistical properties of $\langle SEY \rangle$ considering W_{max} uncertainties $\sigma_r = 5, 10, 30\%$.

- The data in Table 8 shows that μ of $\langle SEY \rangle$ and $\langle SEY \rangle_{error}$ remain relatively similar across distributions for each different σ_r of W_{max}, so it can be concluded that the uncertainty of W_{max}, ranging from $\sigma_r = 5\%$ to 30%, does not significantly change the multipacting threshold. This implies that the W_{max} parameter has a minor impact on multipacting, making it the least effective parameter among those considered.
- However, normal distributions of these different σ_r, produce more dispersion of $\langle SEY \rangle$ as indicated by σ and Var.

σ_r of SEY_{max}	Distribution type	Expansion degree	μ of $\langle SEY \rangle$	$\langle SEY \rangle_{error}$	σ of $\langle SEY \rangle$	Var of $\langle SEY \rangle$
5%	Uniform	5	1.0072	0.06	3.10E-04	5.59E–07
	Normal	3	1.0085	0.19	8.30E-04	2.30E–05
	Truncated normal	3	1.0082	0.16	2.84E-04	6.24E–06
10%	Uniform	6	1.0085	0.19	0.0013	1.78E–06
	Normal	4	1.0084	0.18	0.0065	4.17E–05
	Truncated normal	4	1.0077	0.11	0.0014	1.96E–06
30%	Uniform	7	1.0105	0.39	0.0020	4.19E–06
	Normal	4	1.0147	0.81	0.0266	7.06E–04
	Truncated normal	4	1.0110	0.44	0.0035	1.21E–05

Table 7. Statistical quantities of $\langle SEY \rangle$or different σ_r of SEY_{max} with different distributions.

σ_r of W_{max}	Distribution type	Expansion degree	μ of $\langle SEY \rangle$	$\langle SEY \rangle_{error}$	σ of $\langle SEY \rangle$	Var of $\langle SEY \rangle$
5%	Uniform	3	1.0066	0.002	0.0011	6.03E–07
	Normal	3	1.0075	0.09	0.0027	7.07E–06
	Truncated normal	3	1.0062	0.04	6.89E-04	4.74E–07
10%	Uniform	4	1.0061	0.05	0.0012	1.23E–06
	Normal	3	1.0049	0.16	0.0026	6.80E–06
	Truncated normal	3	1.0048	0.17	2.45E-04	5.98E–08
30%	Uniform	5	1.0064	0.02	0.0026	4.46E–06
	Normal	4	1.0087	0.21	0.0029	8.25E–06
	Truncated normal	4	1.0062	0.04	9.29E-04	8.64E–07

Table 8. Statistical quantities of $\langle SEY \rangle$ for different σ_r of W_{max} with different distributions.

Uncertainty propagating of ⟨SEY⟩ by univariate analyzes

Figure 5 shows the uncertainty of ⟨*SEY*⟩ values (σ_r of ⟨*SEY*⟩) due to the uncertainties of three input parameters: W_1, SEY_{max} and W_{max}. The plots a, b and c represent three different $\sigma_r = 5, 10, 30\%$ respectively. Each block in the plots corresponds to an input parameter and contains 3 bars for the three distributions examined: normal, uniform and truncated normal distributions. The bars show the σ_r of ⟨*SEY*⟩ corresponding to each input parameter with different distributions.

- According to the Fig. 5, we can see that σ_r in W_1 has a significantly larger contribution to the σ_r of ⟨*SEY*⟩ compared to SEY_{max} and W_{max}, indicating that W_1 is the most influential parameter.
- Fig. 5 also shows that the modelling of input parameter uncertainties (σ_r) using different distributions (normal, uniform or truncated Normal) leads to different σ_r of ⟨*SEY*⟩.This means that the distribution type of the input parameter affects ⟨*SEY*⟩ uncertainty.
- For any of three input parameters and any σ_r, the normal distribution causes higher uncertainty of ⟨*SEY*⟩ compared to the uniform and the truncated normal distributions.
- The Uniform and Truncated Normal distributions lead to relatively similar σ_r of ⟨*SEY*⟩.

Bivariate uncertainty quantification results

This section investigates the impact of joint uncertainties in two input parameters simultaneously on the multipacting threshold. To conduct this analysis, we use bivariate gPC method. This allows for a more comprehensive analysis compared to considering parameter uncertainties individually. So in the following, the result of the joint uncertainties between W_{max} & W_1, SEY_{max} & W_1, and W_{max} & SEY_{max} on the ⟨*SEY*⟩ are provided respectively.

Uncertainty of W_1 & W_{max}

First, we assume SEYmax to be a constant value of 2.3. Using the bivariate gPC method, we calculate the ⟨*SEY*⟩ considering the $\sigma_r = 5, 10, 30\%$ of W_1 and Wmax simultaneously. Subsequently, we compute the corresponding ⟨*SEY*⟩ values and present the statistical quantities in Table 9.

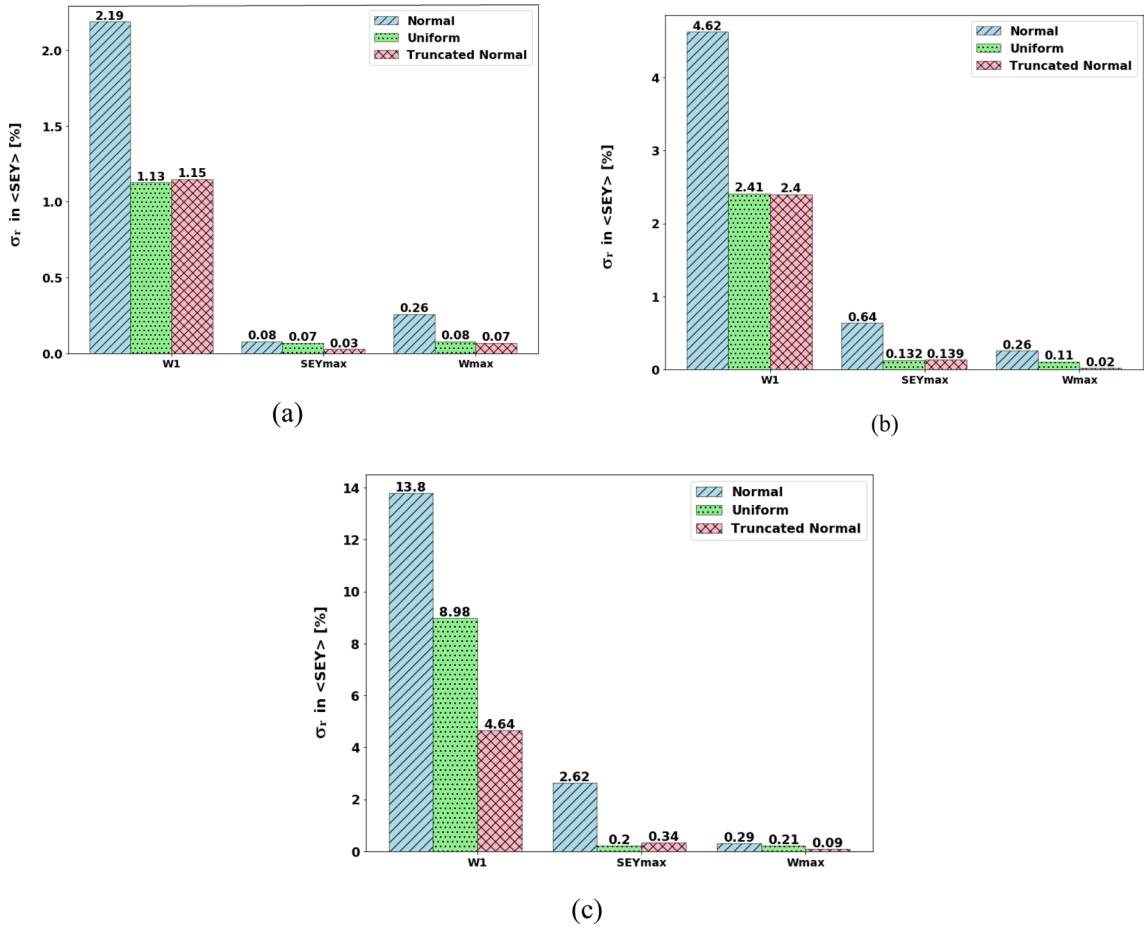

Figure 5. σ_r of ⟨*SEY*⟩, due to the σ_r of the input parameters with three different distributions (**a**) $\sigma_r = 5\%$ of the input parameters (**b**) $\sigma_r = 10\%$ of the input parameters (**c**) $\sigma_r = 30\%$ of the input parameters.

σ_r in W_1&W_{max}	Distribution type	Expansion degree	μ of $\langle SEY \rangle$	$\langle SEY \rangle_{error}$	σ of $\langle SEY \rangle$	Var of $\langle SEY \rangle$
5%	Uniform	5	1.0066	0.001	1.48E−04	5.13E−04
	Normal	4	1.0063	0.03	0.0222	4.91E−04
	Truncated normal	4	1.0061	0.05	0.0121	1.47E−04
10%	Uniform	6	1.0078	0.12	0.0302	5.27E−04
	Normal	5	1.0119	0.53	0.0391	0.0015
	Truncated normal	5	1.0079	0.13	0.0215	4.63E−04
30%	Uniform	7	1.0301	2.34	0.0725	0.0053
	Normal	6	1.0398	3.30	0.1422	0.0202
	Truncated normal	6	1.0092	0.26	0.0758	5.75E−3

Table 9. Statistical quantities of $\langle SEY \rangle$ values for different σ_r in, W_1 & W_{max} with different distribution.

- According to Table 9 the multipacting threshold remains unchanged for $\sigma_r = 5\%$ with the three distributions for W_1 & W_{max}. For $\sigma_r = 10\%$ for two parameters, the multipacting threshold changes with normal distribution, but remains unchanged with uniform and truncated normal distributions. For $\sigma_r = 30\%$, μ of $\langle SEY \rangle$ changes for both normal and uniform distributions of inputs, but remains unchanged for truncated normal distribution.
- The standard deviation (σ) and variance (Var) of $\langle SEY \rangle$ for truncated normal distribution of W_1 &W_{max} are similar to that for the uniform distributions for the three different of σ_r, and have higher values for normal distribution.

For two parameters, W_1 & W_{max}, the first and second order Sobol sensitivity indices were computed, taking into account $\sigma_r = 30\%$ applied simultaneously to the W_1&W_{max} with the three different distributions.

- According to Fig. 6, W_1 has a significantly larger impact on $\langle SEY \rangle$ compared to the Wmax, ($S_{W_1} >> S_{W_{max}}$). This indicates that deviations of W_1 have a greater effect on the multipacting threshold than that of W_{max}.
- For the normal and uniform distributions, S_{W1} values are almost the same, $S_{W_1\,(Uniform)} \cong S_{W_1\,(Normal)}$, suggesting that the variation of W_1 with different distributions does not significantly affect $\langle SEY \rangle$
- Similarly, $S_{W_{max}}$ are also close for both distributions, i.e. $S_{W_{max}\,(Uniform)} \cong S_{W_{max}\,(Normal)}$. Small value of $S_{W_{max}}$ indicates that the variation of $\langle SEY \rangle$ is not strongly affected by the choice of distributions σ_r for W_1 & W_{max}.
- However, the second-order Sobol index ($S_{w_1,w_{max}}$), which shows the effects of interaction between two parameters on the $\langle SEY \rangle$, is higher for the normal distribution that for the uniform distribution This suggests that the normal distribution exhibits stronger effect of the parameters interaction on $\langle SEY \rangle$ than the uniform distributions.

Uncertainty of W_1 & SEY_{max}

Here we assume W_{max} to be constant at 380 eV. Using the bivariate gPC method, we calculate the $\langle SEY \rangle$ considering the combined uncertainties in W_1 & SEY_{max} for different σ_r (See Table 10).

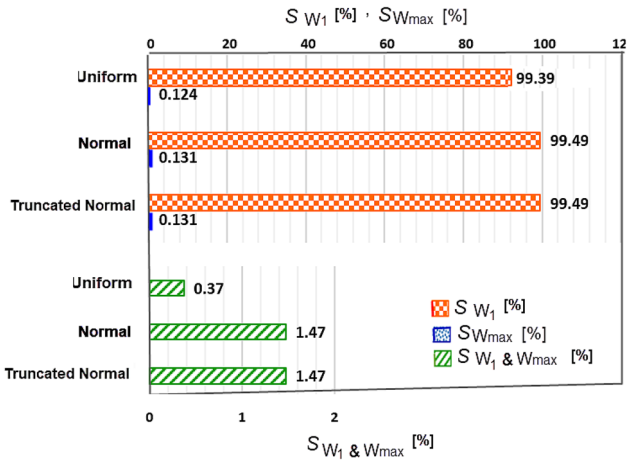

Figure 6. Result of Sobol indices for $\sigma_r = 30\%$ applied simultaneously to the W_1&W_{max} with three distributions.

σ_r in W_1,SEY_{max}	Distribution type	Expansion degree	μ of $\langle SEY \rangle$	$\langle SEY \rangle_{error}$	σ of $\langle SEY \rangle$	Var of $\langle SEY \rangle$
5%	Uniform	3	1.0077	0.11	0.0118	1.39E–04
	Normal	3	1.0046	0.19	0.0234	5.47E–04
	Truncated normal	3	1.0061	0.05	0.0118	1.39E–04
10%	Uniform	5	1.0049	0.16	0.0250	6.24E–04
	Normal	4	1.0079	0.13	0.0402	0.0016
	Truncated normal	4	1.0082	0.16	0.0215	4.63E–04
30%	Uniform	5	1.0156	0.90	0.0743	0.0055
	Normal	5	1.0258	1.91	0.1237	0.0179
	Truncated normal	5	1.0125	0.59	0.0720	0.0052

Table 10. Statistical quantities of $\langle SEY \rangle$ for different σr of W_1& SEY_{max} with different distributions.

- Based on the μ of $\langle SEY \rangle$ in the Table 10, it is observed that for $\sigma_r = 5$, 10% for W_1 & W_{max}, the $\langle SEY \rangle$ remains unchanged for any of the three distributions. However, as σ_r increases up to 30%, the $\langle SEY \rangle$ changes in the normal and truncated normal distributions while remaining unchanged in the uniform distribution.
- Furthermore, the standard deviation (σ) and variance (Var) of $\langle SEY \rangle$ for the truncated normal distribution of W_1 & W_{max} are nearly similar to the uniform distribution and smaller than the normal distribution.

For two parameters, W_1 & SEY_{max}, the first and second order Sobol sensitivity indices are computed, taking into account $\sigma_r = 30\%$ with the three different distribution.

- According to Fig. 7, W_1 has a significantly larger influence on $\langle SEY \rangle$ compared to the SEY_{max}, ($S_{W_1} > S_{SEY_{max}}$). This indicates that deviations in W_1 have a greater effect on the multipacting threshold than deviations of SEY_{max}.
- The results also show that for $\sigma_r = 30\%$ in W_1&SEY_{max} parameters with a uniform distribution, S_{W_1} is higher than normal distribution, $S_{w_1(Uniform)} > S_{w_1(Normal)}$, on the other hand $S_{SEY_{max}}$ for the uniform distribution of σ_r in W_1& SEY_{max}, has a lower value than their normal distribution, $S_{SEY_{max}(Uniform)} < S_{SEY_{max}(Normal)}$. The second-order Sobol index of these two parameters ($S_{W_1,SEY_{max}}$) for the normal distribution is higher than their uniform distribution,$S_{W_1,SEY_{max}(Normal)} > S_{W_1,SEY_{max}(Uniform)}$.

Uncertainty in SEY_{max} & W_{max}
In this section we keep $W_1 = 22$ eV constant and for various σ_r, the bivariate gPC method is used to calculate the $\langle SEY \rangle$ function considering the joint uncertainties in SEY_{max} & W_{max}. The corresponding $\langle SEY \rangle$ values are then computed, and the statistical quantities are presented in Table 11.

- Based on the μ of $\langle SEY \rangle$ in the Table 11, it is observed that for $\sigma_r = 5$, 10% in SEY_{max} & W_{max}, $\langle SEY \rangle$ remains unchanged for any of the three distributions. However, as the σ_r increases up to 30%, $\langle SEY \rangle$ changes with the three different distributions.
- Furthermore, the standard deviation (σ) and variance (Var) of $\langle SEY \rangle$ for the truncated normal distribution of SEY_{max} & W_{max} are nearly similar to the uniform distribution and smaller than their normal distribution.

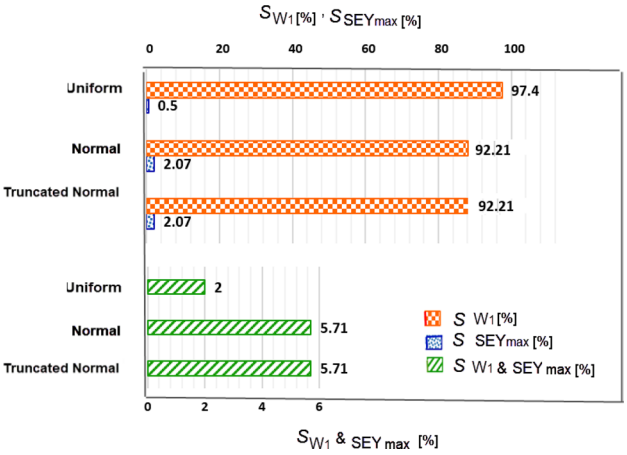

Figure 7. Result of Sobol indices for $\sigma_r = 30\%$ applied simultaneously to the W_1&SEY_{max} with three distributions.

σ_r in SEY_{max}, W_{max}	Distribution type	Expansion degree	μ of $\langle SEY \rangle$	$\langle SEY \rangle_{error}$	σ of $\langle SEY \rangle$	Var of $\langle SEY \rangle$
5%	Uniform	5	1.0068	0.02	8.62E-04	7.44E−07
	Normal	3	1.0064	0.02	4.37E-04	1.91E−07
	Truncated normal	3	1.0060	0.06	0.00067	4.46E−07
10%	Uniform	4	1.0066	0.001	0.0022	4.69E−06
	Normal	4	1.0066	0.001	0.0039	1.57E−05
	Truncated normal	4	1.0060	0.06	0.0010	1.04E−06
30%	Uniform	6	1.0124	0.58	0.0020	1.44E−06
	Normal	5	1.0130	0.64	0.0052	2.68E−05
	Truncated normal	5	1.0104	0.38	0.0721	5.18E−03

Table 11. Statistical quantities of $\langle SEY \rangle$ for different σr in SEYmax &Wmax with different distributions.

For two parameters, SEY_{max} & W_{max}, the first and second order of Sobol sensitivity indices are computed, taking into account $\sigma_r = 30\%$ with the three different distributions.

- Results in Fig. 8 show that SEY_{max} has a larger influence on $\langle SEY \rangle$ compared to the W_{max}, ($S_{SEY_{max}} > S_{W_{max}}$).
- The results show that for $\sigma_r = 30\%$ of W_1&SEY_{max} parameters with the uniform distribution, $S_{SEY_{max}}$ is higher than that with the normal distribution ($S_{SEY_{max}(Uniform)} > S_{W_{max}(Normal)}$).But on the other hand $S_{W_{max}}$ for the uniform distribution of σ_r of W_1& SEY_{max}, has a lower value than that for their normal distribution ($S_{SEY_{max}(Uniform)} < S_{W_{max}(Normal)}$). The second-order Sobol index of these two parameters ($S_{SEY_{max},W\,max}$) for the normal distribution is higher than that for the uniform distribution ($S_{SEY_{max},W_{max}(Normal)} > S_{SEY_{max},W_{max}(Uniform)}$).

Uncertainty propagating of $\langle SEY \rangle$ by bivariate analyzes

Figure 9 shows the σ_r (uncertainty created) of $\langle SEY \rangle$ resulting from the simultaneous uncertainty of the input parameters (W_1 & W_{max}), (W_1 & SEY_{max}), and (SEY_{max} & W_{max}) using three different distributions. The three values of uncertainty $\sigma_r = 5\%$, 10%, and 30% were considered and the results are presented in the figures (a), (b), and (c), respectively.

Figure 9 shows that in the bivariate cases, with σ_r of the normal distribution for the combination of two parameters, σ_r of the multipacting threshold is higher. Additionally, these results indicate that the σ_r of $\langle SEY \rangle$ is nearly the same for the simultaneous changes in the pair of input parameters (W_1&W_{max}) and (W_1&SEY_{max}).

Determining the allowable deviation range of SEY parameters

The findings presented in this article indicate that parameter W_1 has the most significant impact on the multipactor threshold. The uncertainty contribution of this parameter is notably higher compared to the other two parameters. Furthermore, the Sobol sensitivity index for W_1 is larger than that for the other parameters, suggesting that even a small variation of W_1 can lead to a substantial deviation of the multipacting threshold. To determine the permissible range of SEY parameter deviations that would ensure no change of the multipacting

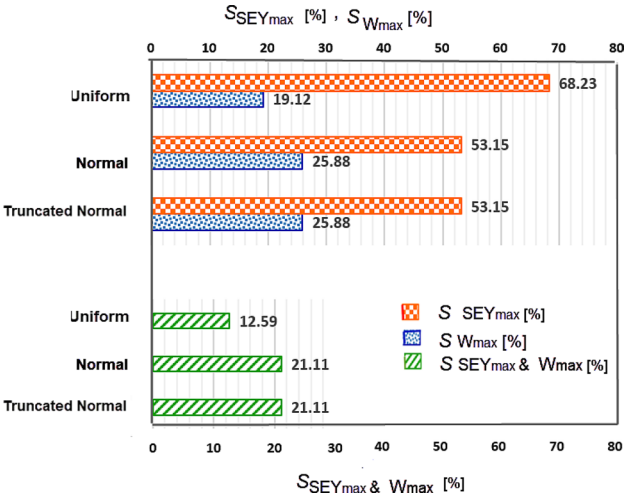

Figure 8. Result of Sobol indices for the $\sigma_r = 30\%$ applied simultaneously to the SEY_{max} & W_{max} with three different distributions.

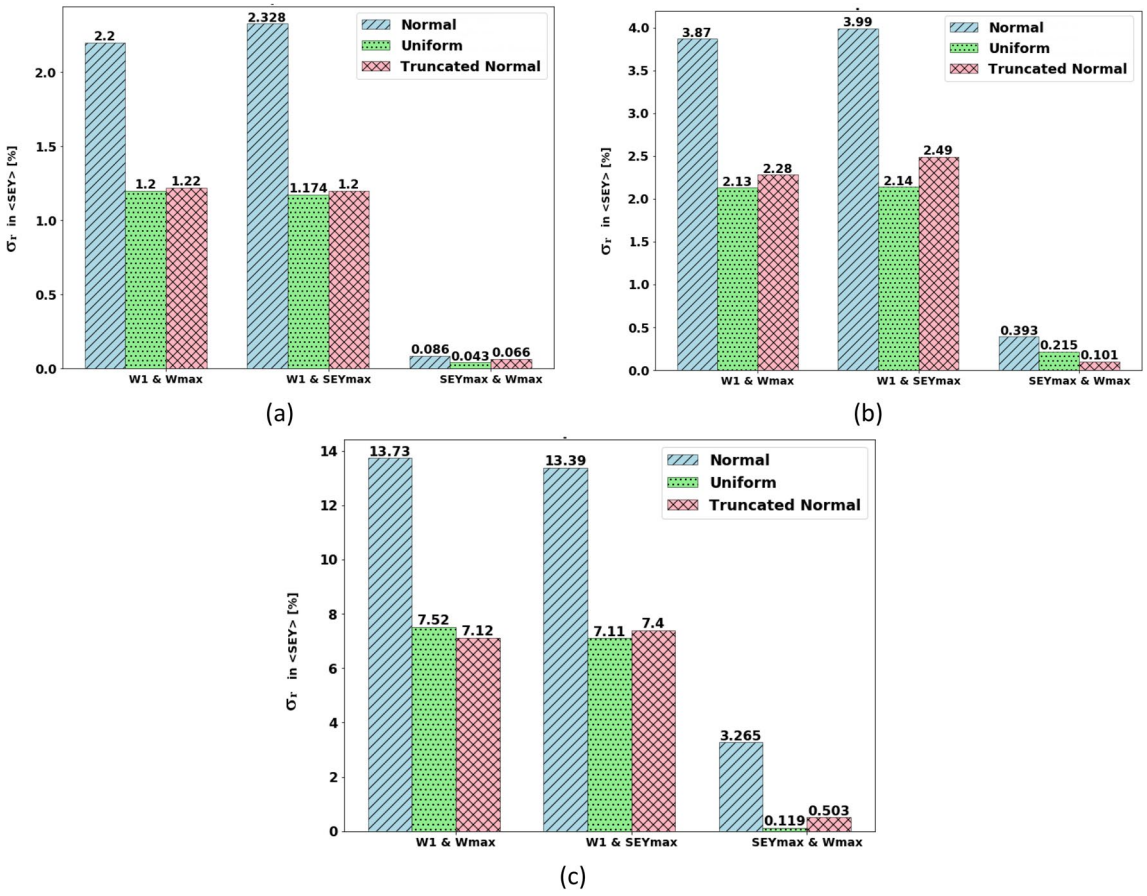

Figure 9. σ_r created in $\langle SEY \rangle$ (uncertainty created in $\langle SEY \rangle$ for the applying simultaneous σ_r in the input joint parameters (W_1&W_{max}), (W_1&SEYmax) and (SEY_{max} & W_{max}) with three different distributions (**a**) $\sigma_r = 5\%$ in inputs, (**b**) $\sigma_r = 10\%$ in inputs (**c**) $\sigma_r = 30\%$ in inputs.

threshold, we focused solely on exploring deviations of the W_1 parameter. Specifically, we examined deviations of 15% and 20% in W_1 to determine the extent of deviations at which multipacting does not occur.

The $\langle SEY \rangle$ for $\sigma_r = 15\%$ and 20% in W_1 for the three different distributions are given in the Table 12.

$\langle SEY \rangle$ does not change for $\sigma_r = 15\%$ in W_1, and it remains relatively constant for three different distributions. However, when σ_r increases to 20%, the μ of $\langle SEY \rangle$ for the uniform and normal distributions increase, leading to the multipacting occurrence. Therefore, we can conclude that deviations of up to 15% are acceptable for SEY parameter uncertainty.

Conclusion

The aim of this study was to investigate the effect of different distributions of uncertainty (σ_r) of the SEY parameters (W_1, W_{max}, and SEY_{max}) on the uncertainty of the multipacting threshold i.e. $\langle SEY \rangle$.

According to the result, the different uncertainty distributions for the SEY parameters result in varying predictions for the multipacting threshold. The choice of distribution for the input parameters is important. For instance, when σ_r of W_1 is equal to 30%, the normal distribution predicts the occurrence of multipacting, whereas both the uniform and the truncated normal distribution indicate its absence.

σ_r in W_1	Distribution type	μ of $\langle SEY \rangle$
15%	Uniform	1.0074
	Normal	1.0080
	Truncated normal	1.0063
20%	Uniform	1.014
	Normal	1.019
	Truncated normal	1.0082

Table 12. Statistical quantities of $\langle SEY \rangle$ for $\sigma_r = 15$, 20% in W_1 with three different distributions.

The investigation also reveals that the choice of random distribution for SEY parameters significantly affects the dispersion of $\langle SEY \rangle$. The standard deviation (σ) and variance (Var) consistently show higher dispersion for the normal distribution compared to the other two distributions. On the other hand, the truncated normal distribution of $\langle SEY \rangle$ results in lower values of $\langle SEY \rangle$ and less variability compared to variability of the uniform and normal distributions. This difference can be attributed to the inherent characteristics of the normal distribution, such as symmetry and tails extending to infinity, which contribute to larger deviations in the $\langle SEY \rangle$ values compared to the truncated normal and the uniform distributions.

The investigation reveals that the uncertainty of W_1 has a more substantial impact on the uncertainty of $\langle SEY \rangle$ in comparison to the other two parameters, (W_{max} and SEY_{max}). Furthermore, when examining the uncertainty of W_1 together with either W_{max} or SEY_{max}, their contributions to the overall uncertainty are almost equal. This observation can be explained by the significant influence of W_1 on the outcome.

Based on the results obtained from Sobol's sensitivity indices analysis, it can be concluded that the choice of different distributions significantly affects Sobol's sensitivity indices. The second-order sensitivity index assesses how the interaction between two SEY parameters influences the value of $\langle SEY \rangle$.

Comparing scenarios where parameters follow normal or uniform distributions, we observe that the second-order index yields higher values when normal distributions are used. It follows that parameters with normal distributions tend to exhibit stronger interactions, and this interaction has a greater effect on multipacting threshold variations. When uncertainty and errors in one parameter are reduced, uncertainty and errors in the other parameter may also be reduced. Controlling variations in the multipacting threshold thus becomes less costly and computationally intensive.

On the contrary, parameters with uniform distributions, which are more widely spread, might not interact so significantly. Therefore, the choice of parameter distribution becomes crucial, since it significantly affects our interpretation of Sobol indices. These indices, in turn, help us comprehend the relative impact of each parameter. When dealing with models involving multiple input parameters, the selection of parameter distribution becomes crucial as it directly affects the accuracy of the analysis and the results of Sobol indices.

Choosing an appropriate distribution for modeling uncertainties in a given model depends on the specific characteristics of the required data and the conditions of the case being studied. In this specific study, it appears that the truncated normal distribution is a suitable choice for modeling the uncertainty of SEY parameters. This choice is based on the following reasons:

- According to the reference[35], the results with the truncated normal distribution for the parameters of a physical model are closer to the calculated theoretical values.
- In the truncated normal and normal distributions, the expansion coefficients and the approximation of the function are calculated using the Gauss-Hermit quadrature, which provides lower error compared to that of for the uniform distribution and Clenshaw-Curtis quadrature.
- The computation cost of expansion coefficients in the normal distribution is less than that in the uniform distribution. This is because the number of nodes in the Gaussi-Hermit quadrature method for the normal distribution is fewer than the nodes in the Clenshaw-Curtis quadrature method for the uniform distribution, consequently, the number of simulations for calculating < SEY > using the CST is reduced.
- The truncated normal distribution shows less change of $\langle SEY \rangle$ values and its dispersion, and does not have outlier data that cause incorrect prediction of the threshold compared to the normal distribution.

The consideration of the simultaneous uncertainty of three parameters (W_1, SEY_{max} and W_{max}) may provide more comprehensive results, and the correlations between them may be significant. However, undoubtedly, this comes at a higher computational cost. Therefore, the current study does not specifically address the three-variable case in order to manage computational resources efficiently.

Data availability

The data that supports the findings of this study are available within the article.

Received: 4 September 2023; Accepted: 3 January 2024
Published online: 08 January 2024

References

1. Lin, S. *et al.* Quantitative analysis of multipactor threshold sensitivity to secondary emission yield of microwave devices. *Phys. Plasmas* https://doi.org/10.1063/5.0138875 (2023).
2. Mirmozafari, M., Behdad, N. & Booske, J. H. Ultrawideband, high-power, microstripline test setup for experimental study and characterization of multipactor. *Rev. Sci. Instrum.* https://doi.org/10.1063/5.0058049 (2021).
3. Langellotti, S. V., Jordan, N. M., Lau, Y. Y. & Gilgenbach, R. M. Multipactor experiments on an S-band coaxial test cell. *Rev. Sci. Instrum.* https://doi.org/10.1063/5.0074464 (2021).
4. Vdovicheva, N. K., Sazontov, A. G. & Semenov, V. E. Statistical theory of two-sided multipactor. *Radiophys. Quantum Electron.* **47**, 580–596 (2004).
5. Yang, H., Huang, W., Zeng, B. & Wen, H. An analytical method to evaluate the spectrum of multicarrier multipactor discharge. *IEEE Trans. Electron. Devices* **68**, 1918–1923 (2021).
6. Siddiqi, M. & Kishek, R. A. A predictive model for two-surface multipactor stability and growth based on chaos theory. *Phys. Plasmas* https://doi.org/10.1063/1.5126275 (2019).
7. Zhang, X., Chang, C. & Gimeno, B. Multipactor analysis in circular waveguides excited by TM01 mode. *IEEE Trans. Electron. Devices* **66**, 4943–4951 (2019).
8. Furman, M. A. & Pivi, M. T. F. Probabilistic model for the simulation of secondary electron emission. *Phys. Rev. Spec. Top. Accel. Beams* **5**, 82–99 (2002).

9. Vaughan, R. Briefs secondary emission formulas. *IEEE Trans. Electron. Devices* **40**, 830 (1993).
10. Sombrin, J. Claquage Hyperfréquence Et Effet Multipactor Dans Les Satellites. *OHD93, Publ. results have been obtained with Sombrin TEEY Model* (1993).
11. Malik, T., Gilmore, M., Portillo, S. & Schamiloglu, E. Secondary electron yield measurements on materials of interest to vacuum electron communication devices. In *2020 IEEE 21st International Conference on Vacuum Electronics, IVEC 2020* (2020). https://doi.org/10.1109/IVEC45766.2020.9520541.
12. Wang, J., Sian, T., Valizadeh, R., Wang, Y. & Wang, S. The effect of air exposure on SEY and surface composition of laser treated copper applied in accelerators. *IEEE Trans. Nucl. Sci.* **65**, 2620–2627 (2018).
13. Petit, V., Taborelli, M., Neupert, H., Chiggiato, P. & Belhaj, M. Role of the different chemical components in the conditioning process of air exposed copper surfaces. *Phys. Rev. Accel. Beams* https://doi.org/10.1103/PhysRevAccelBeams.22.083101 (2019).
14. Vaughan, J. R. M. Some high-power window failures. *IRE Trans. Electron. Devices* **8**, 302–308 (1961).
15. Gilmour, A. S. Jr. *Microwave Tubes* (Artech House, 1986).
16. Yamaguchi, S., Michizono, S. & Anami, S. Trajectory simulation of multipactoring electrons in an S-band pillbox RF window. *IEEE Trans. Nucl. Sci.* **39**, 278–282 (1992).
17. Kobayashi, S., Michizono, S. & Anami, S. Surface flashover on alumina RF windows for high-power use. *IEEE Trans. Electr. Insul.* https://doi.org/10.1109/14.231539 (1993).
18. Kishek, R. A. & Lau, Y. Y. Multipactor discharge on a dielectric. *Phys. Rev. Lett.* **80**, 193–196 (1998).
19. Zhang, X., Yu, Q. & Ni, X. Saturation mechanism of multipactor effect in a one-sided dielectric-loaded waveguide. *IEEE Trans. Electron. Devices* **69**, 748–753 (2022).
20. Wen, D. Q., Zhang, P., Krek, J., Fu, Y. & Verboncoeur, J. P. Higher harmonics in multipactor induced plasma ionization breakdown near a dielectric surface. *Phys. Rev. Lett.* https://doi.org/10.1103/PhysRevLett.129.045001 (2022).
21. Silvestre, L. *et al.* A continuum approach for multipactor using Vlasov-Poisson analysis. *J. Phys. D Appl. Phys.* **55**, 045202 (2022).
22. Lin, S., Sun, P., Li, Y., Wang, H. & Liu, C. Enhanced multipactor statistical modeling for accurate threshold prediction with numerically tracking electron trajectories. *Phys. Plasmas* https://doi.org/10.1063/1.5133955 (2020).
23. Belfio, J., Lazar, F., Belhaj, M. & Jbara, O. Low electron emission yield electrodeposited silver coating for electron multipacting mitigation. *Surf. Interfaces* **37**, 102651 (2023).
24. Mostajeran, M., Tulu, E. T. & van Rienen, U. Uncertainty in the isosceles multipactor threshold of triangularly grooved surfaces based on polynomial chaos. *Nucl. Instrum. Methods Phys. Res. Sect. A Accel. Spectrom. Detect. Assoc. Equip.* **993**, 165001 (2021).
25. Kazemi, F., Mostajeran, M. & Romanov, G. The influence of secondary electron yield uncertainty on the single-sided multipacting in dielectrics. *Eur. Phys. J. Plus* https://doi.org/10.1140/epjp/s13360-023-04124-9 (2023).
26. Fil, N., Belhaj, M., Hillairet, J. & Puech, J. Erratum: Multipactor threshold sensitivity to total electron emission yield in small gap waveguide structure and TEEY models accuracy (Phys. Plasmas (2016) 23 (123118) DOI: 10.1063/1.4972571). *Phys. Plasmas* **27**, 069902 (2016).
27. Ghanem, R. G. & Spanos, P. D. *Stochastic Finite Elements: A Spectral Approach* (Courier Corporation, 1991). https://doi.org/10.1007/978-1-4612-3094-6.
28. Liorni, I., Parazzini, M., Fiocchi, S. & Ravazzani, P. Study of the influence of the orientation of a 50-Hz magnetic field on fetal exposure using polynomial chaos decomposition. *Int. J. Environ. Res. Public Health* **12**, 5934–5953 (2015).
29. Schmidt, C., Member, S., Grant, P., Lowery, M. & Rienen, U. V. Influence of uncertainties in the material properties of brain tissue on the probabilistic volume of tissue activated. *IEEE Trans. Biomed. Eng.* **60**, 1378–1387 (2013).
30. Litvinenko, A., Logashenko, D., Tempone, R., Wittum, G. & Keyes, D. Propagation of uncertainties in density-driven flow. *Lect. Notes Comput. Sci. Eng.* **144**, 101–126 (2021).
31. Barthelmann, V., Novak, E. & Ritter, K. High dimensional polynomial interpolation on sparse grids. *Adv. Comput. Math.* **12**, 273–288 (2000).
32. Grzelak, L. A., Witteveen, J. A. S., Suárez-Taboada, M. & Oosterlee, C. W. The stochastic collocation Monte Carlo sampler: highly efficient sampling from 'expensive' distributions. *Quant. Financ.* **19**, 339–356 (2019).
33. Eck, V. G. *et al.* A guide to uncertainty quantification and sensitivity analysis for cardiovascular applications. *Int. J. Numer. Method. Biomed. Eng.* https://doi.org/10.1002/cnm.2755 (2016).
34. Berutti, P., Khabiboulline, T. & Romanov, G. *Multipactor discharge in the pip-ii superconducting spoke resonators* (2014).
35. Kazemi, F. & Mostajeran, M. How do different distributions of random input have an effect on output results in a simulated physical. *J. Stat. Model. Theory* **3**, 123–134 (2023).

Author contributions

F.K. Conducted the simulation, performed statistical analysis of results, and drafted the initial manuscript. M.M. Generated the fundamental concept and idea for the article, substantially enhanced the article's content in terms of scientific rigor and writing quality. G.R. Improved the simulation portion of the research, Implemented necessary corrections to enhance the overall quality of the article.

Competing interests

The authors declare no competing interests.

Additional information

Supplementary Information The online version contains supplementary material available at https://doi.org/10.1038/s41598-024-51289-z.

Correspondence and requests for materials should be addressed to M.M.

Reprints and permissions information is available at www.nature.com/reprints.

Publisher's note Springer Nature remains neutral with regard to jurisdictional claims in published maps and institutional affiliations.